JCTC Journal of Chemical Theory and Computation

All-Electron Scalar Relativistic Basis Sets for the Lanthanides

Dimitrios A. Pantazis and Frank Neese*

Lehrstuhl für Theoretische Chemie, Institut für Physikalische und Theoretische Chemie, Universität Bonn, Wegelerstrasse 12, D-53115 Bonn, Germany, and Max-Planck-Institut für Bioanorganische Chemie, Stiftstrasse 34-36, 45470 Mülheim an der Ruhr, Germany

Received February 22, 2009

Abstract: Segmented all-electron relativistically contracted (SARC) basis sets are constructed for the elements $_{57}$La−$_{71}$Lu and optimized for density functional theory (DFT) applications. The basis sets are intended for use in combination with the DKH2 or ZORA scalar relativistic Hamiltonians for which individually optimized contractions are provided. Significant computational advantages can be realized owing to the loose contraction of the SARC basis sets compared to generally contracted basis sets, while their compact size allows them to replace effective core potentials for routine studies of lanthanide complexes. The new basis sets are evaluated in DFT calculations of the first four ionization energies of the lanthanides. They yield results that accurately reproduce the experimental trends, confirming a balanced treatment of different electronic configurations. The performance of the basis sets is further assessed in molecular systems with a comprehensive study of the lanthanide trihalides. Despite their compact size, the SARC basis sets demonstrate consistent, efficient, and reliable performance and will be especially useful in calculations of molecular properties that require explicit treatment of the core electrons.

Introduction

Despite the traditional "rare earth" misnomer, the elements La−Lu that comprise the 4f block of the periodic table are ubiquitous in nature and are more abundant, in fact, than many transition metals.[1] Owing to their special chemical and physical properties, they are similarly ubiquitous in practical applications and occupy a central place in modern science and technology. Lanthanide complexes find extensive use as catalysts in synthetic chemistry,[2,3] but in general their applications are more often associated with their unique optical and magnetic properties stemming from the partially occupied 4f shell.[4] Thus, they feature prominently in the area of molecular magnetism, especially in the rapidly expanding field of d/f heterometallic chemistry.[5−8] They are of fundamental importance in the technology of lasers, the fabrication of special glasses, and the construction of cathode-ray or plasma displays as well as in the materials for light emitting diodes and optical fibers.[9] In the biomedical field, the luminescence of lanthanides is exploited for labeling purposes in biological assays[10] and nanoparticle bioprobes.[11,12] Lanthanide compounds are also actively researched for therapeutic uses,[13] while the most highlighted application in clinical practice is arguably the dominant use of gadolinium(III) complexes as contrast agents in magnetic resonance imaging.[14−16]

From a quantum chemical perspective, the lanthanides present difficulties in their computational treatment because of the large number of electrons and the necessity to account for significant relativistic effects.[17] In many practical cases, such as in density functional theory (DFT)[18,19] studies of structures and relative energies, both of these issues can be addressed by the use of effective core potentials (ECPs), which are adjusted to reproduce relativistic reference data that go beyond most approximate Hamiltonians.[20] By explicitly treating only the valence electrons, ECPs also serve to decrease the computational requirements while simulta-

* Corresponding author. E-mail: neese@thch.uni-bonn.de.

10.1021/ct900090f CCC: $40.75
Published on Web 08/12/2009

neously incorporating scalar relativistic effects implicitly through parametrization. Note, however, that the definition of "valence electrons" is not obvious for the lanthanides. There are mainly three types of effective core potentials and associated valence basis sets available for lanthanides. These include the averaged relativistic ECPs and the spin−orbit operators of Ross et al. with a [Xe] core,[21] the shape-consistent quasirelativistic ECPs of Cundari and Stevens with a [Kr]d^{10} core,[22] and the energy-consistent quasirelativistic ECPs and basis sets of Dolg,[23−29] which come in a "large-core" (the 4f shell is included in the core) and a "small-core" variety that treats the four, five, and six shell electrons explicitly. In contrast to their heavier 5f congeners, the partially occupied 4f shell of the lanthanides can, for many purposes, be considered as chemically inert and, thus, can be subsumed into the ECP. Even though this eliminates most of the magnetic and electronic subtleties of the lanthanides, it has proven to give acceptable results in studies that focus on the structural features or the estimates of relative energies.[30,31] However, this approach requires a separate potential for each oxidation state or 4f configuration[29] and, in practice, it precludes the modeling of f-centered processes and the treatment of spin−orbit coupling, while it may also mask the potential effects of f shell asphericity on structure.[32]

Thus, the use of large-core ECPs has inherent limitations, and one is faced with the dilemma that reducing the size of the core will allow for a more flexible treatment of the valence region, whereas a larger core allows for a better modeling of the all-important relativistic effects. Deficiencies of ECPs have been pointed out in specific situations. A recent example is the systematic study of the spin-state energies of iron complexes by Swart and co-workers, who showed that the use of ECPs results in spin-state splittings that never converge to the common limit attainable by both Slater- and Gaussian-type all-electron basis sets, regardless of the extension of the valence basis.[33] In a different field of application, Frenking and co-workers have noted that total electron densities derived from ECP calculations are associated with artifacts in the topological analysis.[34] From the field of molecular magnetism, a recent theoretical study of the exchange coupling in Gd^{III}/Cu^{II} systems by Cirera and Ruiz addressed the performance of different relativistic approaches and basis sets, concluding that effective core potentials lead to qualitatively incorrect results; only the combination of the all-electron basis sets with a scalar relativistic Hamiltonian proved capable of producing the correct behavior.[35] All these examples highlight the need for reliable and efficient all-electron alternatives to ECPs, a requirement that is also fundamental when properties of the inner shells are being probed, as in EPR or X-ray absorption experiments.

Thus, either for validating the use of ECPs or circumventing some of their limitations, it is necessary to have all-electron basis sets that allow efficient calculations with the popular scalar relativistic Hamiltonians, such as the zeroth order regular approximation[36−38] (ZORA), the infinite order regular approximation[39] (IORA), and the Douglas−Kroll−Hess[40−44] (DKH) approach. It should be emphasized that nonrelativistic basis sets are not flexible enough in the core region to be used with scalar relativistic Hamiltonians. Besides, even if used completely uncontracted, standard basis sets lack the much higher exponents that are typically required by scalar relativistic Hamiltonians. To the best of our knowledge, existing Slater-type scalar relativistic all-electron basis sets for the lanthanides are limited to the ZORA basis sets available in the Amsterdam density functional code.[45,46] Gaussian-type all-electron relativistic basis sets for the lanthanides include the atomic natural orbital (ANO-RCC) basis sets of Roos et al. for use with the DKH2 Hamiltonian,[47] the DKH3 basis sets of Hirao and co-workers, which are available for both point- and finite-nucleus approximations,[48,49] and the segmented contracted correlating basis sets of Koga and co-workers.[50] These three families of large and high-quality basis sets are suitable for use with correlated ab initio methods and, in combination with such theoretical approaches, are able to deliver highly accurate results for small systems.[47−50] However, their size and construction is not tailored to the more modest requirements of DFT approaches, which show much faster convergence for molecular properties with respect to extension of the basis set.[18] A more serious issue in terms of efficiency for the Roos and Hirao basis sets is their general contraction, since for DFT calculations the generation of two-electron integrals over basis functions dominates the computational effort.

Hence, we feel that it is important to have small standard Gaussian basis sets available that are not generally contracted and are compact enough to be used in day-to-day DFT calculations with the most popular scalar relativistic Hamiltonians. In this paper, we propose such segmented all-electron relativistically contracted (SARC) basis sets, which are constructed for DFT treatments of lanthanide systems in conjunction with the scalar relativistic DKH or ZORA Hamiltonians. The SARC basis sets are sufficiently small in terms of the total number of basis functions so as not to present a grossly inefficient alternative to ECPs for routine DFT studies of large molecules. Exponents of the Gaussian primitives are derived from relatively simple empirical rules, and contraction coefficients are determined separately for both the ZORA and second-order DKH (DKH2) schemes. These two scalar relativistic approximations produce quite distinct shapes for the core orbitals,[51] therefore, the contractions must be adapted to each particular Hamiltonian. The same strategy has been used successfully in the construction of SARC basis sets for third-row transition metals[51] and has been extensively evaluated in calibration studies of first-, second- and third-row transition metal geometries.[52] All the above basis sets are now part of the freely available ORCA program package.[53] The performance of the SARC basis sets is assessed here for both atomic and molecular properties.

Construction of Basis Sets. Restricted open-shell Hartree−Fock (ROHF) calculations were first carried out for each atom in its ground-state configuration in order to obtain the innermost radial expectation values that are subsequently employed in the generation of the new primitive Gaussian functions. These calculations followed Zerner's spin-averaged (SAHF) formalism,[54,55] as implemented in ORCA.[53] Within this approach, the ROHF code averages over all of

Table 1. Radial Expectation Values of Innermost Orbitals (in Bohr) Determined from Spin-Averaged ROHF Calculations

	$\langle r_s \rangle$	$\langle r_p \rangle$	$\langle r_d \rangle$	$\langle r_f \rangle$
La	0.026644	0.097171	0.259694	
Ce	0.026180	0.095340	0.253476	0.983364
Pr	0.025731	0.093569	0.247552	1.008485
Nd	0.025298	0.091867	0.241922	0.960901
Pm	0.024879	0.090226	0.236554	0.920354
Sm	0.024473	0.088641	0.231428	0.884966
Eu	0.024081	0.087111	0.226529	0.853546
Gd	0.023701	0.085636	0.221853	0.783083
Tb	0.023333	0.084202	0.217344	0.813301
Dy	0.022976	0.082819	0.213034	0.793152
Ho	0.022629	0.081480	0.208898	0.773551
Er	0.022293	0.080184	0.204925	0.754670
Tm	0.021967	0.078927	0.201104	0.736583
Yb	0.021651	0.077709	0.197427	0.719308
Lu	0.021343	0.076531	0.193896	0.674575

the states of a given spin for a given configuration. Although Huzinaga's decontracted well-tempered basis sets (WTBS)[56,57] were found to be perfectly adequate for this step, in the case of third-row transition metal atoms,[51] exploratory calculations indicated that a larger basis set would be needed to approach the basis set limit for the lanthanides. Therefore, in this work we have chosen the universal Gaussian basis set (UGBS) of de Castro and Jorge.[58,59] We extended the number of primitive Gaussian functions beyond the range proposed in the original paper in order to create a common basis set that covers consistently all elements with $Z = 57-71$. This led to a (34s24p20d14f) basis set which was used in a completely decontracted form, resulting in 304 functions per atom. We note that this basis set (referred to simply as UGBS in the following) yields total atomic energies that deviate less than 1 mE_h from the nonrelativistic numerical Hartree−Fock values of Koga et al.[60] and, thus, can serve as a suitable reference point for benchmarking. All atoms were considered in their respective ground states; these generally arise from $4f^n6s^2$ configurations with the exception of La, Ce, Gd, and Lu, which have an electron in the 5d shell. In detail, the atomic configurations and ground states are: La ($5d^16s^2$, ^{2}D), Ce ($4f^15d^16s^2$, ^{1}G), Pr ($4f^36s^2$, ^{4}I), Nd ($4f^46s^2$, ^{5}I), Pm ($4f^56s^2$, ^{6}H), Sm ($4f^66s^2$, ^{7}F), Eu ($4f^76s^2$, ^{8}S), Gd ($4f^75d^16s^2$, ^{9}D), Tb ($4f^96s^2$, ^{6}H), Dy ($4f^{10}6s^2$, ^{5}I), Ho ($4f^{11}6s^2$, ^{4}I), Er ($4f^{12}6s^2$, ^{3}H), Tm ($4f^{13}6s^2$, ^{2}F), Yb ($4f^{14}6s^2$, ^{1}S), and Lu ($4f^{14}5d^16s^2$, ^{2}D). The resulting radial expectation values $\langle r_l \rangle$ of the 1s, 2p, 3d, and 4f orbitals are listed in Table 1.

Following the same procedure as previously detailed,[51] the exponents α_l of the tightest s, p, d, and f functions were determined from the radial expectation values as $\alpha_l = 2k_l f_l^2/\pi\langle r_l \rangle^2$, where $f_l = 1$, 4/3, 8/5, and 64/35 for $l =$ s, p, d, and f. Scaling factors k_l of 1 000, 100, 33, and 10 were used for s, p, d, and f functions, respectively. The exponents of these tightest basis functions per atom are listed in Table 2. Notice the regular and smooth variation of the exponents along the series, which implies that the basis sets could be used reliably for comparisons between systems containing different lanthanide atoms. Sets of primitive Gaussians were then constructed for each angular momentum as series of the form $\alpha_i x^{-i}$ ($i = 1, 2, ...$), $x = 2.25$, 2.50, 2.75, and 3.00 for $l =$ s, p, d, and f. Exponent cutoff values were set to 0.02 for s, p, and d functions and 0.2 for f functions, but more diffuse functions can be easily generated from the same formula. We emphasize that the above values for the empirical extrapolation factors x were found to serve well our primary goal of a sufficiently small number of functions that still maintain high performance in terms of atomic and molecular properties, while also ensuring fast convergence for DFT calculations. Of course, a choice of larger values for x can lead to more densely spaced primitives, if this need arises in special applications.

Table 2. Maximum Exponents Per Angular Momentum (in Bohr^{-2}) Used for the Construction of the SARC Basis Sets

	α_s	α_p	α_d	α_f
La	896770.416684	11986.275399	797.462366	
Ce	928839.847608	12451.087955	837.067226	22.012804
Pr	961538.755282	12926.877106	877.609164	20.929801
Nd	994735.795984	13410.301051	918.931840	23.054021
Pm	1028523.650946	13902.541106	961.110752	25.130098
Sm	1062932.540176	14404.172125	1004.158396	27.180085
Eu	1097819.871374	14914.599562	1048.060643	29.217975
Gd	1133304.941480	15432.804306	1092.706223	34.712700
Tb	1169335.032050	15962.936347	1138.514896	32.181136
Dy	1205955.486947	16500.520028	1185.048662	33.836944
Ho	1243224.036239	17047.298098	1232.439088	35.573458
Er	1280982.187936	17602.816491	1280.690360	37.375741
Tm	1319284.994791	18167.970032	1329.819235	39.233820
Yb	1358076.401925	18741.957799	1379.815234	41.140939
Lu	1397555.920017	19323.367785	1430.527887	46.778199

The resulting uncontracted basis sets have the form (23s16p12d6f) comprising 173 primitives in total (131 for La since no f functions are used). In the last step, the innermost six s, five p, four d, and four f primitives were contracted to create the final basis sets with a [18s12p9d3f] pattern and 120 functions. To put this number into perspective, the uncontracted (26s23p17d13f) ANO-RCC basis sets[47] would yield 271 functions, while the (27s23p15d10f) Hirao basis sets[48] correspond to 241 functions. On the other hand, the valence [10s8p5d4f] basis set of Dolg's small-core ECP basis[27] already contains 87 contracted basis functions. Contraction coefficients were obtained by scalar relativistic calculations of the atomic ground states and are specifically optimized for each scalar relativistic Hamiltonian (DKH2 or ZORA). These SARC basis sets are of valence triple-ζ (TZV) quality, and in molecular calculations employing the DKH2 or ZORA Hamiltonians, they should normally be combined with their relativistically contracted counterparts for the other atoms, either the respective SARC basis sets for the third-row transition metals or the appropriate relativistically contracted variants of the Karlsruhe basis sets[51] for other elements that are freely available in the ORCA basis set library. Additional basis functions of higher angular momentum to be used as polarization or correlation functions were generated by scaling the most diffuse existing exponents by 1.25. One additional function has been used for TZVP and three functions for TZVPP-quality basis sets. Complete listings of the basis sets in ready-to-use format are provided in the Supporting Information.

Assessment and Applications. *Evaluation of Basis Set Construction.* Compared to the large uncontracted UGBS, two formal approximations enter in the construction of the new SARC basis sets: the significant reduction in the total

Table 3. Estimated Incompleteness Errors (E_h) from Comparison of the UGBS and SARC Basis Sets[a]

	UGBS (304 functions)	SARC (120 functions)	ΔE
La	–8486.519526	–8485.444981	1.074545
Ce	–8853.276583	–8851.937575	1.339008
Pr	–9229.684172	–9228.320549	1.363623
Nd	–9615.948651	–9614.439880	1.508771
Pm	–10012.152291	–10010.488169	1.664122
Sm	–10418.434516	–10416.603845	1.830671
Eu	–10834.936141	–10832.926564	2.009578
Gd	–11261.687283	–11259.548746	2.138537
Tb	–11698.581889	–11696.151822	2.430067
Dy	–12146.284756	–12143.621665	2.663092
Ho	–12604.772058	–12601.859229	2.912829
Er	–13074.195242	–13071.014408	3.180834
Tm	–13554.708332	–13551.239799	3.468533
Yb	–14046.468030	–14042.690360	3.777670
Lu	–14549.587004	–14545.604380	3.982623

[a] Spin-averaged ROHF calculations with the DKH2 Hamiltonian.

number of primitives and the contraction of the innermost functions in a specific pattern adapted to the scalar relativistic Hamiltonians. Thus, the magnitude of the errors introduced by the above approximations, namely the incompleteness and contraction error, can serve as a preliminary indicator for the internal consistency and construction quality of the SARC basis sets.

In order to determine these errors, we performed SAHF calculations with the DKH2 Hamiltonian for the atomic ground states. In Table 3 we compare the total electronic energies obtained with the [18s12p9d3f] SARC basis sets to those obtained with the (34s24p20d14f) UGBS, the latter being considered a good approximation to the basis set limit. The energy difference is a good estimate of the incompleteness error, which rises monotonically from 1.07 E_h for lanthanum up to 3.98 E_h for lutetium. The effect of contraction is, of course, folded into the incompleteness error, as determined above. Therefore, to obtain an estimate of the contraction error, additional calculations were performed using the SARC basis sets in fully uncontracted form (23s16p12d6f). The difference in the total energies obtained by the contracted and uncontracted SARC versions is found to increase smoothly from a minimum of 33 mE_h for lanthanum to a maximum of 74 mE_h for lutetium, clearly a minor effect compared to the magnitude of the incompleteness error.

The small values and the limited span of both the incompleteness and the contraction errors are remarkable. To appreciate this point we have to refer to the SARC basis sets for the third-row transition metals,[51] which have already been shown to be of excellent quality in practical applications.[52] In that case, the basis sets displayed incompleteness errors ranging from a little over 4.22 up to 7.75 E_h, all values beyond the corresponding error range for the lanthanides. Furthermore, the maximum contraction error in the present case is lower than the lowest contraction error obtained for a third-row transition metal (hafnium, at 79 mE_h). Although incompleteness and contraction errors are not expected to significantly influence molecular properties other than total energies, these fundamental metrics already demonstrate the quality of the proposed basis sets in terms of both size and contraction pattern.

Table 4. Bond Lengths r (pm) and Dissociation Energies D_e (eV) of Lanthanide Diatomics Computed with the DKH2 Hamiltonian, without and with BSSE Counterpoise Corrections (CPC), Compared with Experiment

	PBE0/SARC		PBE0/SARC+CPC		expt[a]	
	r	D_e	r	D_e	r	D_e
LaH ($^1\Sigma$)	202.1	2.57	202.2	2.57	203.2	–
LaF ($^1\Sigma$)	203.0	6.43	203.0	6.40	202.7	6.23
LaO ($^2\Sigma$)	184.2	7.82	184.3	7.80	182.6	8.29
LuH ($^1\Sigma$)	190.3	3.12	190.4	3.12	191.2	3.47
LuF ($^1\Sigma$)	191.3	7.22	191.4	7.20	191.7	5.93[b]
LuO ($^2\Sigma$)	178.1	6.84	178.1	6.81	179.0	7.04

[a] Refs 63 and 64. [b] Estimated.

Nevertheless, it is possible that the existing incompleteness error might give rise to basis set superposition errors in molecular calculations if the incompleteness arises from an insufficient description of the valence orbitals. To clarify this point, we have performed DKH2 calculations with the PBE0 functional on a series of lanthanide hydrides, fluorides, and oxides using the two elements at the ends of the series (La and Lu). The def2-TZVP basis sets were used for H, F, and O. The bond length and dissociation energy of each species were corrected for BSSE errors using the counterpoise correction method of Boys and Bernardi.[61] The results (Table 4) indicate that superposition errors are either minimal or nonexistent, the corrections being at the most 0.1 pm for the bond lengths and 0.03 eV for the dissociation energies. Therefore, the valence orbitals that contribute to the bonding appear to be covered quite well with the SARC basis sets, and thus, the incompleteness error is not associated with the valence space. Note that these conclusions may only hold for DFT, where basis set completeness for the valence space is relatively easy to achieve. Correlated ab initio methods typically require larger and more extensively polarized basis sets than the basis sets proposed here.[62]

In terms of basis set performance for atomic systems, another useful descriptor is the energy of the outermost valence and semicore orbitals (6s, 5d, and 4f) compared to the essentially converged UGBS results. Using the data obtained from the SA-ROHF DKH2 calculations described in the previous section, we observe a very close agreement between the SARC and the UGBS results. Specifically, the energies of the 6s orbitals are practically identical, with maximum deviations of 0.01 eV. For the four elements that have an occupied 5d orbital in their ground-state configuration (La, Ce, Gd, and Lu), the 5d energies also agree within 0.03 eV. Greater discrepancies are observed for the energies of the 4f orbitals, which are stabilized with the SARC basis sets by 0.30 eV on average, but this difference is still too small to cause any concern about the performance of the basis sets in routine molecular applications. These observations are in line with the comments made above regarding the coverage of the valence space and the minimal BSSE errors, and they also confirm that the incompleteness errors reported in Table 3 are not associated with the valence orbitals.

The origin of the incompleteness errors is discovered upon moving close to the nucleus, where the difference in size of the two basis sets leads to more pronounced deviations in

Table 5. Orbital Energies (E_h) and Radial Expectation Values for Lutetium, Obtained from SAHF-DKH2 Calculations with the UGBS and SARC Basis Sets

	UGBS		SARC			
	E	<*r*>	*E*	<*r*>	Δ*E*	Δ<*r*>
1s	–2334.889	0.019	–2334.342	0.019	0.547	0.000
2s	–402.623	0.081	–402.713	0.081	–0.090	0.000
2p	–355.307	0.072	–355.434	0.072	–0.128	0.000
3s	–93.381	0.212	–93.513	0.212	–0.132	0.000
3p	–78.819	0.211	–78.949	0.211	–0.129	0.000
3d	–60.730	0.192	–60.854	0.193	–0.124	0.000
4s	–19.664	0.479	–19.729	0.479	–0.065	0.000
4p	–14.769	0.507	–14.820	0.507	–0.051	0.000
4d	–8.151	0.549	–8.186	0.550	–0.035	0.000
5s	–2.697	1.194	–2.705	1.192	–0.008	–0.002
5p	–1.439	1.408	–1.442	1.406	–0.004	–0.002
4f	–0.822	0.701	–0.816	0.705	0.006	0.004
6s	–0.222	3.910	–0.222	3.905	0.000	–0.005
5d	–0.188	2.739	–0.188	2.742	0.000	0.003

absolute energies, with the most part of the discrepancy attributed to the chemically unimportant 1s orbital. It is possible to reduce the discrepancy by using higher s exponents, but this creates imbalances in other shells and introduces numerical instabilities that can be typically avoided with a finite-nucleus model.[49] Regardless, this energy difference is chemically irrelevant. For the DFT applications the SARC basis sets are aimed at, we cannot think of any situation where convergence to a "basis set limit" scalar relativistic energy would be sought. For such purposes, other methods and basis sets mentioned in the introduction might present better options. The most relevant criterion here is the radial expectation value because this better reflects the scalar relativistic effects that the basis sets aim to capture. Importantly, for all core and semicore orbitals there is coincidence in the $\langle r \rangle$ values. Table 5 presents detailed orbital energies and radial expectation values for the "worst-case" element, lutetium. Based on the properties of atomic orbitals, we conclude that the SARC basis sets are overall well-balanced for their size, yielding orbital features that follow those predicted by the significantly larger UGBS basis set both close to the core and in the valence space.

Ionization Energies. The first ionization energies (IE_1) of the lanthanides are known with high accuracy (within 0.02 eV), and this makes them ideal for benchmarking the new basis sets for atomic systems in a more rigorous way. We evaluate ionization energies using the B3LYP functional as a representative DFT method, since it is one of the typical hybrid functionals to be used in the expected application setting of the SARC basis sets. Across all lanthanides, and similar to the 5d transition series, the first ionization energy is associated with the removal of an electron from the doubly occupied 6s orbital except for lutetium, which loses the single 5d electron to attain a closed-shell configuration. In the case of cerium, a change of configuration is observed with an increase of the 5d occupation number. As expected from the semicore character of the 4f orbitals, their occupation remains intact. Thus, the specific configurations and corresponding ground states of the cations are: La^+ ($5d^2$, ^3F), Ce^+ ($4f^15d^2$, ^4H), Pr^+ ($4f^36s^1$, ^5I), Nd^+ ($4f^46s^1$, ^6I), Pm^+ ($4f^56s^1$, ^7H), Sm^+ ($4f^66s^1$, ^8F), Eu^+ ($4f^76s^1$, ^9S), Gd^+ ($4f^75d^16s^1$, ^{10}D), Tb^+ ($4f^96s^1$, ^7H), Dy^+ ($4f^{10}6s^1$, ^6I), Ho^+ ($4f^{11}6s^1$, ^5I), Er^+ ($4f^{12}6s^1$, ^4H), Tm^+ ($4f^{13}6s^1$, ^3F), Yb^+ ($4f^{14}6s^1$, ^2S), and Lu^+ ($4f^{14}6s^2$, ^1S). Note that the ground state of the Ce atom ($4f^15d^16s^2$, ^1G) is a non-Hund (or "unnatural parity") singlet state, as discussed in depth by Morgan and Kutzelnigg,[65] and as such, it is inaccessible within the current DFT framework. Thus, the triplet state of the neutral Ce atom was used instead for our B3LYP calculation of ionization energies. As anticipated, our results confirm that this pragmatic choice is the logical one for the DFT approach and has no adverse effect on computed quantities.

Table 6. First Ionization Energies (eV) Computed with the B3LYP Functional and the Uncontracted UGBS Basis Set, with and without Relativistic Corrections, Compared with Experimental Values

		nonrelativistic		DKH2		ZORA	
	expt[a]	IE_1	Δ*E*	IE_1	Δ*E*	IE_1	Δ*E*
La	5.58	4.80	–0.78	5.56	–0.02	5.57	–0.01
Ce	5.54	5.02	–0.52	5.46	–0.08	5.47	–0.07
Pr	5.47	5.16	–0.31	5.39	–0.08	5.40	–0.07
Nd	5.52	5.21	–0.31	5.45	–0.07	5.46	–0.06
Pm	5.58	5.25	–0.33	5.51	–0.07	5.52	–0.06
Sm	5.64	4.34	–1.30	5.57	–0.07	5.57	–0.07
Eu	5.67	5.33	–0.34	5.62	–0.05	5.63	–0.04
Gd	6.15	7.06	0.91	6.07	–0.08	6.08	–0.07
Tb	5.86	5.48	–0.38	5.81	–0.05	5.82	–0.04
Dy	5.94	5.55	–0.39	5.92	–0.02	5.93	–0.01
Ho	6.02	5.61	–0.41	6.01	–0.01	6.02	0.00
Er	6.11	5.68	–0.43	6.11	0.00	6.12	0.01
Tm	6.18	5.74	–0.44	6.19	0.01	6.21	0.03
Yb	6.25	5.80	–0.45	6.28	0.03	6.29	0.04
Lu	5.43	6.56	1.13	5.39	–0.04	5.39	–0.04
MAD			0.56		0.05		0.04
rms			0.64		0.05		0.05

[a] Reference 66.

Before we assess the SARC basis sets, it is instructive to see how large is the importance of scalar relativistic effects for this property using the practically complete UGBS basis set. According to the B3LYP results presented in Table 6, nonrelativistic calculations generally underestimate ionization energies with a root-mean-squared (rms) error of 0.64 eV. Interestingly, this error is significantly smaller than that obtained from similar nonrelativistic calculations for the third-row transition metal atoms (1.39 eV). This rms value, however, masks the fact that pronounced nonsystematic failures, such as the qualitatively different ionization process for Gd ($f^8d^1s^1$ to $f^7d^2s^0$ compared with the relativistic $f^7d^1s^2$ to $f^7d^1s^1$), lead to a wide error spread of more than 2.4 eV. Inclusion of scalar relativistic effects with either the DKH2 or the ZORA Hamiltonians produces an evidently more uniform behavior and reduces the rms error down to only 0.05 eV.

In view of the large difference in size between the UGBS and the SARC basis sets (304 and 120 basis functions, respectively), we anticipated that moving to the more compact SARC basis sets might adversely affect the accuracy of the calculated values. However, the results summarized in Table 7 show that the reduction in size, which is accompanied by significant gains in terms of computational cost, does not compromise in any way the accuracy of the

Table 7. First Ionization Energies (eV) Computed with the B3LYP Functional and the SARC Basis Sets, Compared with Experimental Values

		DKH2		ZORA	
	expt[a]	IE_1	ΔE	IE_1	ΔE
La	5.58	5.58	0.00	5.59	0.01
Ce	5.54	5.54	0.00	5.54	0.00
Pr	5.47	5.41	–0.06	5.42	–0.05
Nd	5.52	5.47	–0.05	5.47	–0.05
Pm	5.58	5.52	–0.06	5.53	–0.05
Sm	5.64	5.58	–0.06	5.59	–0.05
Eu	5.67	5.63	–0.04	5.64	–0.03
Gd	6.15	6.08	–0.07	6.09	–0.06
Tb	5.86	5.80	–0.06	5.81	–0.05
Dy	5.94	5.93	–0.01	5.94	0.00
Ho	6.02	6.02	0.00	6.03	0.01
Er	6.11	6.13	0.02	6.13	0.02
Tm	6.18	6.20	0.02	6.22	0.04
Yb	6.25	6.29	0.04	6.30	0.05
Lu	5.43	5.39	–0.04	5.39	–0.04
MAD			0.04		0.03
rms			0.04		0.04

[a] Reference 66.

Table 8. Second, Third, and Fourth Ionization Energies (eV) Computed with the B3LYP Functional and the SARC Basis Sets using the DKH2 Hamiltonian, Compared with Experimental Values

	IE_2		IE_3		IE_4	
	calc	expt[a]	calc	expt[a]	calc	expt[a]
La	11.23	11.06	19.15	19.17	50.63	49.94
Ce	10.72	10.85	20.45	20.20	37.14	36.76
Pr	10.80	10.55	21.77	21.62	38.94	38.98
Nd	10.97	10.73	22.48	22.08	40.82	40.41
Pm	11.14	10.90	22.91	22.28	41.77	41.15
Sm	11.30	11.07	24.13	23.42	42.42	41.35
Eu	11.45	11.24	25.18	24.92	43.93	42.60
Gd	12.36	12.09	20.45	20.62	44.76	44.05
Tb	11.77	11.52	22.22	21.91	40.95	39.79
Dy	11.86	11.67	23.30	22.80	42.30	41.47
Ho	11.99	11.80	23.49	22.84	43.60	42.60
Er	12.12	11.93	23.48	22.74	43.93	42.65
Tm	12.25	12.05	24.50	23.68	44.04	42.69
Yb	12.38	12.19	25.41	25.03	45.26	43.74
Lu	14.03	13.89	21.27	21.07	45.74	45.19
MAD	0.21		0.41		0.86	

[a] Reference 1.

predicted ionization energies. The rms error is even marginally reduced by 0.01 eV, testifying to the well-balanced construction of the basis sets. It should be pointed out that the present all-electron B3LYP/SARC results compare very favorably with previously published high-level calculations of the first ionization energies of lanthanides. For example, multireference averaged coupled-pair functional (ACPF) calculations employing relativistic energy-consistent small-core pseudopotentials[24] with extensive valence basis sets of up to 114 functions achieved mean absolute deviations (MAD) in the range of 0.22−0.24 eV,[26,27] and more recent CASPT2 calculations with the ANO-RCC basis sets achieve an accuracy around 0.1 eV.[47]

For a more comprehensive evaluation of the SARC basis sets, we present the second, third, and fourth ionization energies of the lanthanide atoms in Table 8, computed with the B3LYP and the DKH2 Hamiltonian. Compared with the results obtained for IE_1, larger deviations are observed as successive electrons are removed, with a tendency toward overestimation of ionization energies. Nevertheless, the computed values are still satisfactory and compare well with the results of Cao and Dolg,[26] exactly matching the ACPF accuracy for the chemically most relevant third ionization potential. This is obviously of importance for most practical molecular applications, since the lanthanides are normally found in the +3 oxidation state. We emphasize that the experimental uncertainties associated with the ionization energies increase rapidly from IE_2 to IE_4, often exceeding 1 eV for IE_4 in the middle of the series. This, combined with the fact that the present DFT approach might not treat differential correlation effects on an equal footing, complicates the assessment of individual cases for IE_2 to IE_4. In contrast to the actinides, the effects of spin−orbit coupling in the lanthanides are not usually considered of crucial importance for the calculation of ionization energies because they are smaller in magnitude than the differential correlation effects arising from the different electronic configurations.[26,27,47,67] Note, however, that Liu and Dolg have shown that spin−orbit effects may become as large as 0.5 eV toward the end of the series when the f occupancy is changed.[68] Although inclusion of spin−orbit corrections would be necessary for high-accuracy work, especially when higher ionization energies are calculated, for the methods we use here (B3LYP), it is not expected that inclusion of spin−orbit corrections would lead to systematic improvement of the computed values.[26,27,47,67]

Regardless of the origin of specific deviations in absolute numerical values, the diagram of cumulative ionization energies in Figure 1 demonstrates that all experimentally observed trends across the series are faithfully reproduced by the calculations. Ionization energies generally increase from the lighter to the heavier elements, with specific irregularities related to filled and half-filled f subshell effects. The most characteristic deviations from the trend are the low IE_3 values for gadolinium and lutetium, which attain f^7 and f^{14} configurations at the +3 oxidation state, whereas europium and ytterbium display high IE_3 values owing to the loss of an electron from the corresponding f^7 and f^{14} configurations of their +2 state. Removal of a fourth electron is very costly for lanthanum because of its filled p subshell (xenon configuration) in the +3 oxidation state. On the other hand, low IE_4 values create two deep minima in the cumulative diagram for cerium (p^6 at the +4 state) and terbium (f^7 at the +4 state). This agrees perfectly with chemical facts since cerium, with an IE_4 of approximately 36.8 eV (calculated 37.1 eV), is the only element of the series that has extensive chemistry at the +4 oxidation state. Overall, the computed ionization energies closely follow the experimental patterns and do not reveal any bias for a particular electronic configuration, thus reinforcing our confidence in the ability of the SARC basis sets to cover all chemically relevant oxidation states across the entire 4f series.

Geometries of Trihalide Complexes. The lanthanide trihalides (LnX_3) form a complete and fairly well characterized class of compounds that encompass all elements of the

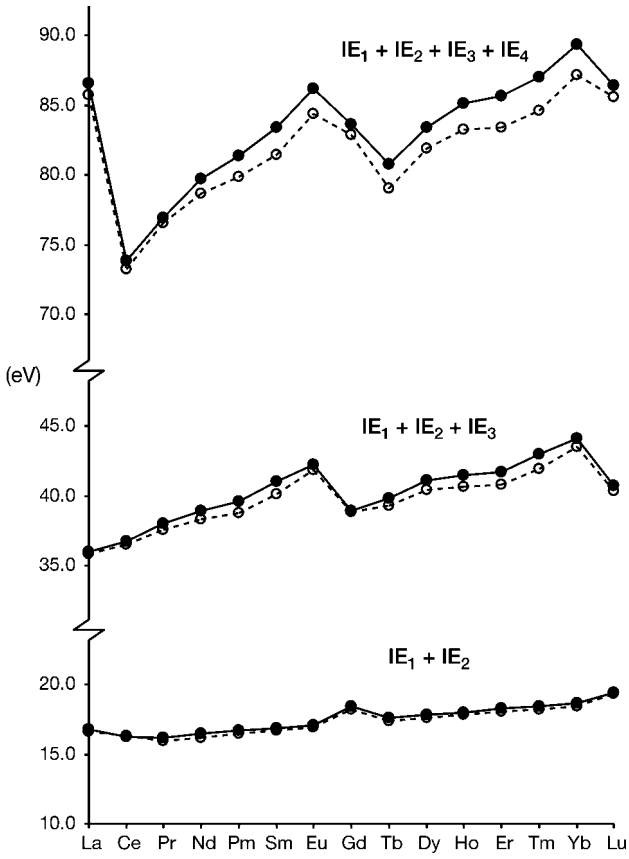

Figure 1. Cumulative ionization energies (eV) of the lanthanide atoms: comparison of experimental (dotted line) and calculated values (solid line). Calculations were performed with the SARC basis sets using the B3LYP functional and the DKH2 Hamiltonian.

4f series;[69] this makes them a suitable reference for testing the performance of the new basis sets with respect to molecular geometries. Several publications presenting theoretical studies of specific members of the family exist, and we refer the reader to the comprehensive review by Kovács and Konings for a detailed overview of the relevant literature.[69] However, to the best of our knowledge, the only study to explicitly address the complete series of lanthanides and halides is that of Cundari et al.,[70] who employed a multiconfigurational (MC) SCF approach with effective core potentials that leave the 4f electrons of the lanthanides in the valence space.[22] Since MCSCF does not attempt to account for dynamic correlation, to make a fair comparison in this paper we will use the same DFT method to compare values obtained with the ECPs and the SARC all-electron basis sets using the DKH2 Hamiltonian. For the ECP calculations, we use the Stuttgart−Bonn small-core (28 electrons in the core) pseudopotentials for the lanthanides[24] combined with the high-quality [10s8p5d4f3g] valence basis sets of Cao and Dolg.[27] We employ the hybrid (25% exact exchange) PBE0 density functional,[71] since this emerged as the top performer for geometries of transition metal complexes in our recent calibration study.[52] In the all-electron calculations, the DKH2 relativistically recontracted TZVP basis sets were used for the halides.[51] No symmetry restrictions were imposed on optimizations. As reference values, we use the recommended equilibrium bond distances proposed by Kovács and Konings in their survey of LnX_3 systems.[69] These values were obtained by a joint analysis of trends in available experimental and theoretical data and are currently regarded as the best available estimates.

Table 9. PBE0/SARC (DKH2) Equilibrium Angles (degrees) of Lanthanide Trifluorides and f-orbital Mulliken Population Analysis

	FLnF angle	f charge	f spin
Ce	113	1.4	1.0
Pr	115	2.4	2.0
Nd	118	3.4	3.0
Pm	120	4.3	4.0
Sm	120	5.3	5.0
Eu	114	6.3	6.0
Gd	117	7.2	6.9
Tb	115	8.2	5.9
Dy	117	9.2	4.9
Ho	120	10.2	3.9
Er	120	11.2	3.0
Tm	120	12.2	2.0
Yb	120	13.2	1.0
Lu	120	14.2	0.0

All Br, I, and Cl compounds are predicted by our PBE0 optimizations to be essentially planar, in agreement with available experimental data that support planar or quasiplanar equilibrium structures for the heavier halides.[69] By contrast, many fluorides converge to pyramidal geometries. Pyramidalization of the trifluoride molecules is a long-standing controversial issue that presents challenges for both experiment and theory. A critical review of experimental studies draws attention to the difficulties and ambiguities associated with the collection and the analysis of data concerning X-Ln-X angles,[69] while the sensitivity of computed parameters used methodological choices has not allowed researchers to reach definitive answers through quantum chemical approaches, either. It is accepted that the degree of pyramidalization in the trihalides depends on a subtle balance of factors that may include the polarizability of the lanthanide, the electronegativity and size of the halide, and the asphericity of the 4f electron shell, as suggested by Molnár and Hargittai.[32] In the case of the fluorides, Kovács and Konings suggest a uniform trend in the F−Ln−F angles with an increase in the Ln atomic number, based on steric considerations. This is at odds with the present PBE0/SARC-DKH2 results, which display marked discontinuities. LaF_3, CeF_3, PrF_3, and NdF_3 optimize to pyramidal geometries, but PmF_3 and SmF_3 are planar; deviations from planarity are again observed for the four subsequent lanthanides (Eu, Gd, Tb, Dy), whereas all trifluorides beyond dysprosium are planar. In Table 9, the angles of all trifluorides are given in detail along with the population analysis for the lanthanide f orbitals, which show a slightly higher occupancy than that expected from the formal ionic model.

We do not wish to place excessive confidence to the results concerning the angles, since this particular parameter is known to be sensitive to methodological choices. However, it is impossible to miss the extraordinary agreement with the predictions of the 4f asphericity model.[32] Considering the shape of the 4f shell, Molnár and Hargittai divided the Ln^{3+} cations into two groups: those with a spherically

Table 10. Equilibrium Bond Distances (pm) of Lanthanide Trihalides: PBE0/ECP and PBE0/SARC (DKH2) Results Compared with the Kovács−Konings Recommended Values

	recommended values[a]				PBE0/ECP				PBE0/SARC			
	F	Cl	Br	I	F	Cl	Br	I	F	Cl	Br	I
Ce	207	252	268	286	209	254	270	292	209	255	270	290
Pr	206	251	266	285	206	252	268	289	207	253	268	288
Nd	205	250	265	284	206	250	266	288	207	252	267	287
Pm	204	249	264	283	205	250	265	287	206	251	265	285
Sm	203	248	263	282	204	249	264	287	204	249	264	285
Eu	202	247	262	281	204	248	265	294	203	249	263	288
Gd	201	245	260	280	201	247	263	285	203	247	262	282
Tb	200	244	259	279	200	245	261	283	201	246	260	280
Dy	199	243	258	278	199	244	259	280	200	245	259	279
Ho	198	242	257	277	199	243	258	279	200	243	258	278
Er	197	241	255	276	199	242	257	278	199	242	257	277
Tm	196	240	254	275	198	241	256	277	198	241	256	276
Yb	195	238	253	274	197	240	255	277	197	240	255	276
Lu	194	237	252	273	196	239	253	275	196	239	254	274

[a] Ref 69; the estimated uncertainty is ± 2 pm.

Table 11. Atomization Energies (eV) of Lanthanide Trihalides: PBE0/SARC (DKH2) Results Compared with Experimental Values

	PBE0/SARC				expt[a]				ΔE			
	F	Cl	Br	I	F	Cl	Br	I	F	Cl	Br	I
Ce	19.8	15.4	13.5	12.5	20.1	15.6	13.6	11.2	–0.3	–0.1	–0.1	1.3
Pr	19.0	14.9	13.0	11.6	19.1	15.2	13.2	10.6	0.0	–0.3	–0.2	1.0
Nd	18.5	14.4	12.5	11.2	19.0	14.5	12.6	9.9	–0.6	–0.1	–0.1	1.3
Pm	17.8	13.7	11.8	10.6								
Sm	16.7	12.5	10.6	9.7	17.3	13.2	11.1	9.1	–0.6	–0.7	–0.5	0.6
Eu	15.8	11.8	10.5	8.8	17.2	13.1	10.8	8.5	–1.4	–1.3	–0.3	0.3
Gd	19.2	15.2	13.3	12.0	19.2	15.1	13.1	10.8	0.0	0.1	0.2	1.2
Tb	18.9	14.9	12.6	11.7	19.0	15.1	12.9	10.7	–0.1	–0.2	–0.3	1.0
Dy	17.9	13.9	11.9	10.7	17.3	14.2	11.8	9.7	0.6	–0.3	0.1	1.0
Ho	17.7	13.7	11.8	10.5	17.2	14.3	11.8	9.4	0.5	–0.6	0.0	1.1
Er	17.6	13.6	11.8	10.3	17.2	14.3	12.1	9.9	0.4	–0.7	–0.3	0.4
Tm	16.8	12.8	10.8	9.5	17.0	13.7	11.1	9.0	–0.3	–0.9	–0.3	0.5
Yb	15.8	11.6	9.9	8.6	16.0	12.4	10.1	7.8	–0.2	–0.8	–0.1	0.8
Lu	19.3	15.4	13.4	12.1	18.4	15.2	12.8	10.7	0.9	0.2	0.6	1.4

[a] Ref 77.

symmetrical or an axially elongated 4f shell, for which no distortion of the LnF_3 compounds from the planar geometry is anticipated (La^{3+}, Pm^{3+}, Sm^{3+}, Gd^{3+}, Er^{3+}, Tm^{3+}, Yb^{3+}, Lu^{3+}), and those with an axially compressed 4f shell, for which pyramidal LnF_3 geometries are expected (Ce^{3+}, Pr^{3+}, Nd^{3+}, Eu^{3+}, Tb^{3+}, Dy^{3+}, Ho^{3+}). Despite the fact that the coincidence between these predictions and the present results is not absolute, we suggest that the level of agreement provides strong support to the notion that a uniform periodicity in bond angles should *not* be expected for the trifluorides.

Focusing now on the bond lengths of the trihalides, the results of our PBE0/SARC-DKH2 optimizations are summarized in Table 10, where they are compared with the recommended values as well as with PBE0/ECP results. With both basis sets, a steady contraction of the Ln−X bond length is predicted with an increasing atomic number in the lanthanide. Both methods also yield almost identical total contractions from CeX_3 to LuX_3, 13−14 pm for the fluorides and 16−17 pm for the heavier halides. For each member of the four halide series, the SARC bond length approaches the Kovács−Konings reference value as closely as the ECP result, illustrating that the same level of accuracy in structural parameters can be expected from either approach. Remarkably, the maximum deviation in the F, Cl, and Br series never exceeds 2 pm. In the case of the iodides, an overestimation of the bond length by approximately 3 pm is evident up to Eu, but after this point the optimized values practically coincide with the reference. A point of particular importance is that the PBE0/SARC mean absolute deviation remains constant at 2 pm regardless of the nature of the halide. This encouraging result highlights the fact that the new basis sets combine well with the relativistically recontracted all-electron basis sets for main group elements that we presented in our previous contribution,[51] ensuring well-balanced and consistent performance not only across the periods but also down the groups of the periodic table.

In order to explore the dependence of the bond lengths on methodological choices, we have repeated the calculations with the nonhybrid (GGA) version of the functional, PBE.[72−74] On the whole, this approach yields similarly good results without significant deterioration compared to those of Table 10 (see Supporting Information), although mean average deviations rise to 2, 4, 4, and 5 pm for the four halide species, respectively. However, two discontinuities appear in the form of pronounced maxima at the europium and ytterbium compounds of all halides, followed by sharp contractions for the subsequent elements gadolinium and lutetium. These abrupt changes can become smaller but in

no case eliminated by extending the halide basis sets, whereas extending the SARC basis set has minimal effect. Hence, we are led to attribute the origin of these discrepancies to the imbalanced treatment of different electronic configurations by the GGA functional and/or its incorrect description of the covalency of the Ln-X bond.[75,76] As shown in Table 10, no such disruptions in the uniform contraction trend appear with the hybrid version of the functional, and only a small hump is noticeable for EuI_3.

Finally, the atomization energies of all species were computed at the same level of theory. The values are compared with experimental atomization energies obtained from Myers[77] in Table 11 and show reasonably good agreement with experiment. The largest deviations are observed for the iodides, where atomization energies are typically overestimated by 1 eV. In contrast, the mean absolute deviations for the F, Cl, and Br series are 0.4, 0.5, and 0.2 eV, respectively. In conclusion, it is clear from the results that a protocol based on the SARC basis sets in combination with the PBE0 functional performs accurately and consistently for the prediction of molecular properties across the lanthanide series.

Summary

Scalar all-electron relativistic (SARC) basis sets have been constructed for the accurate and the affordable treatment of lanthanide systems in conjunction with scalar relativistic Hamiltonians (DKH2 or ZORA). The SARC basis sets are small and compact, so they present a very efficient alternative to effective core potentials in routine DFT studies of chemically relevant systems. Their contraction pattern guarantees their computational efficiency compared to generally contracted relativistic basis sets. Extensive evaluation of the basis sets for the first four atomic ionization potentials of the lanthanides demonstrates that they provide a balanced description of different electronic configurations, not only reproducing the experimental trends but also achieving quantitative accuracy in most cases. Thus, they can be used with confidence for the prediction of energetic properties and the unbiased description of processes involving changes in oxidation state and associated changes in 4f and 5d occupation numbers. Moreover, the excellent results obtained with the SARC basis sets and the PBE0 density functional in a detailed study of the lanthanide trihalides confirm that the applicability of the basis sets can be safely extended to molecular systems. The new basis sets are particularly well suited for the calculation of molecular properties that require or benefit from the explicit treatment of the core electrons. These include not only the study of electron paramagnetic resonance, Mössbauer and X-ray absorption spectra, but also the derivation of electron densities that will be subsequently subjected to topological analysis and the study of the magnetic properties in mixed d/f heterometallic complexes and clusters.

Acknowledgment. We gratefully acknowledge financial support from the DFG priority program 1137 "Molecular Magnetism" and from the Max Planck Society.

Supporting Information Available: Full listings of the SARC basis sets. This material is available free of charge via the Internet at http://pubs.acs.org.

References

(1) Cotton, S. *Lanthanide and Actinide Chemistry*. 2nd ed.; John Wiley & Sons: Chichester, U.K., 2006; p 280.

(2) *Lanthanides: Chemistry and Use in Organic Synthesis. Topics in Organometallic Chemistry*, Kobayashi, S., Ed.; Springer-Verlag: Berlin, Germany, 1999; Vol. 2, p 300.

(3) Imamoto, T. *Lanthanides in Organic Synthesis*. Academic Press: London, 1994; p 160.

(4) Bünzli, J.-C. G.; Piguet, C. *Chem. Soc. Rev.* **2005**, *34*, 1048–1077.

(5) Benelli, C.; Gatteschi, D. *Chem. Rev.* **2002**, *102*, 2369–2387.

(6) Bunzli, J. C. G.; Piguet, C. *Chem. Rev.* **2002**, *102*, 1897–1928.

(7) Sakamoto, M.; Manseki, K.; Okawa, H. *Coord. Chem. Rev.* **2001**, *219*, 379–414.

(8) Winpenny, R. E. P. *Chem. Soc. Rev.* **1998**, *27*, 447–452.

(9) Kido, J.; Okamoto, Y. *Chem. Rev.* **2002**, *102*, 2357–2368.

(10) Matsumoto K.; Yuan, J. G. Lanthanide Chelates as Fluorescent Labels for Diagnostics and Biotechnology. In *Metal Ions in Biological Systems*; Sigel, A., Sigel, H., Eds. Marcel Dekker Inc.: New York, 2003; Vol. 40, pp 191−231.

(11) Shen, J.; Sun, L.-D.; Yan, C.-H. *Dalton Trans.* **2008**, 5687–5697.

(12) Bünzli, J.-C. G. *Chem. Lett.* **2009**, *38*, 104–109.

(13) Fricker, S. P. *Chem. Soc. Rev.* **2006**, *35*, 524–533.

(14) Caravan, P.; Ellison, J. J.; McMurry, T. J.; Lauffer, R. B. *Chem. Rev.* **1999**, *99*, 2293–2352.

(15) Bottrill, M.; Kwok, L.; Long, N. J. *Chem. Soc. Rev.* **2006**, *35*, 557–571.

(16) Hermann, P.; Kotek, J.; Kubicek, V.; Lukes, I. *Dalton Trans.* **2008**, 3027–3047.

(17) Pyykkö, P. *Chem. Rev.* **1988**, *88*, 563–594.

(18) Koch, W.; Holthausen, M. C. *A Chemist's Guide to Density Functional Theory*. 2nd ed.; Wiley-VCH: Weinheim, Germany, 2001; p 300.

(19) Parr, R. G.; Yang, W., *Density-Functional Theory of Atoms and Molecules*. Oxford University Press: Oxford, U.K., 1989; p 352.

(20) Dolg, M. Effective core potentials. In *Modern Methods and Algorithms of Quantum Chemistry*, 2 ed.; Grotendorst, J., Ed. John von Neumann Institute for Computing: Jülich, Germany, 2000; Vol. 3, pp 507−540.

(21) Ross, R. B.; Gayen, S.; Ermler, W. C. *J. Chem. Phys.* **1994**, *100*, 8145–8155.

(22) Cundari, T. R.; Stevens, W. J. *J. Chem. Phys.* **1993**, *98*, 5555–5565.

(23) Dolg, M.; Stoll, H.; Savin, A.; Preuss, H. *Theor. Chem. Acc.* **1989**, *75*, 173–194.

(24) Dolg, M.; Stoll, H.; Preuss, H. *J. Chem. Phys.* **1989**, *90*, 1730–1734.

(25) Dolg, M.; Stoll, H.; Preuss, H. *Theor. Chem. Acc.* **1993**, *85*, 441–450.

(26) Cao, X.; Dolg, M.*J. Chem. Phys.* **2001**, *115*, 7348–7355.

(27) Cao, X.; Dolg, M. *J. Mol. Struct. (THEOCHEM)* **2002**, *581*, 139–147.

(28) Yang, J.; Dolg, M. *Theor. Chem. Acc.* **2005**, *113*, 212–224.

(29) Hülsen, M.; Weigand, A.; Dolg, M. *Theor. Chem. Acc.* **2009**, *122*, 23–29.

(30) Dolg, M.; Stoll, H. Electronic structure calculations for molecules containing lanthanide atoms. In *Handbook of Chemistry and Physics of Rare Earths*, Gschneider, K. A., Eyring, L., Eds.; Elsevier: Amsterdam, The Netherlands, 1996; Vol. 22, pp 607−729.

(31) Frenking, G.; Antes, I.; Böhme, M.; Dapprich, S.; Ehlers, A. W.; Jonas, V.; Neuhaus, A.; Otto, M.; Stegmann, R.; Veldkamp, A.; Vyboishchikov, S. F. *Rev. Comp. Chem.* **1996**, *8*, 63–143.

(32) Molnár, J.; Hargittai, M. *J. Phys. Chem.* **1995**, *99*, 10780–10784.

(33) Güell, M.; Luis, J. M.; Solà, M.; Swart, M. *J. Phys. Chem. A* **2008**, *112*, 6384–6391.

(34) Vyboishchikov, S. F.; Sierraalta, A.; Frenking, G. *J. Comput. Chem.* **1997**, *18*, 416–429.

(35) Cirera, J.; Ruiz, E. *C. R. Chim.* **2008**, *11*, 1227–1234.

(36) van Lenthe, E.; Baerends, E. J.; Snijders, J. G. *J. Chem. Phys.* **1994**, *101*, 9783–9792.

(37) van Lenthe, E.; Snijders, J. G.; Baerends, E. J. *J. Chem. Phys.* **1996**, *105*, 6505–6516.

(38) van Wüllen, C. *J. Chem. Phys.* **1998**, *109*, 392–399.

(39) Dyall, K. G.; van Lenthe, E. *J. Chem. Phys.* **1999**, *111*, 1366–1372.

(40) Douglas, M.; Kroll, N. M. *Ann. Phys.* **1974**, *82*, 89–155.

(41) Hess, B. A. *Phys. Rev. A: At., Mol., Opt. Phys.* **1985**, *32*, 756–763.

(42) Hess, B. A. *Phys. Rev. A: At., Mol., Opt. Phys.* **1986**, *33*, 3742–3748.

(43) Jansen, G.; Hess, B. A. *Phys. Rev. A: At., Mol., Opt. Phys.* **1989**, *39*, 6016–6017.

(44) Wolf, A.; Reiher, M.; Hess, B. A. *J. Chem. Phys.* **2002**, *117*, 9215–9226.

(45) *Amsterdam Density Functional (ADF)*, 2007.01; SCM, Theoretical Chemistry, Vrije Universiteit: Amsterdam, The Netherlands, 2007; http://www.scm.com. Accessed September 10, 2008.

(46) te Velde, G.; Bickelhaupt, F. M.; Baerends, E. J.; Guerra, C. F.; Van Gisbergen, S. J. A.; Snijders, J. G.; Ziegler, T. *J. Comput. Chem.* **2001**, *22*, 931–967.

(47) Roos, B. O.; Lindh, R.; Malmqvist, P.-Å.; Veryazov, V.; Widmark, P.-O.; Borin, A. C. *J. Phys. Chem. A* **2008**, *112*, 11431–11435.

(48) Tsuchiya, T.; Abe, M.; Nakajima, T.; Hirao, K. *J. Chem. Phys.* **2001**, *115*, 4463–4472.

(49) Nakajima, T.; Hirao, K. *J. Chem. Phys.* **2002**, *116*, 8270–8275.

(50) Sekiya, M.; Noro, T.; Miyoshi, E.; Osanai, Y.; Koga, T. *J. Comput. Chem.* **2006**, *27*, 463–470.

(51) Pantazis, D. A.; Chen, X. Y.; Landis, C. R.; Neese, F. *J. Chem. Theory Comput.* **2008**, *4*, 908–919.

(52) Bühl, M.; Reimann, C.; Pantazis, D. A.; Bredow, T.; Neese, F. *J. Chem. Theory Comput.* **2008**, *4*, 1449–1459.

(53) Neese, F. *ORCA - an ab initio, Density Functional and Semiempirical Program Package* , Version 2.6−35 Universität Bonn: Bonn, Germany, 2007.

(54) Stavrev, K. K.; Zerner, M. C. *Int. J. Quantum Chem.* **1997**, *65*, 877–884.

(55) Zerner, M. C. *Int. J. Quantum Chem.* **1989**, *35*, 567–575.

(56) Huzinaga, S.; Kolbukowski, M. *Chem. Phys. Lett.* **1993**, *212*, 260–264.

(57) Huzinaga, S.; Miguel, B. *Chem. Phys. Lett.* **1990**, *175*, 289–291.

(58) Jorge, F. E.; de Castro, E. V. R.; da Silva, A. B. F. *J. Comput. Chem.* **1997**, *18*, 1565–1569.

(59) de Castro, E. V. R.; Jorge, F. E. *J. Chem. Phys.* **1998**, *108*, 5225–5229.

(60) Koga, T.; Watanabe, S.; Thakkar, A. J. *Int. J. Quantum Chem.* **1995**, *54*, 261–263.

(61) Boys, S. F.; Bernardi, F. *Mol. Phys.* **1970**, *19*, 553–566.

(62) Küchle, W.; Dolg, M.; Stoll, H. *J. Phys. Chem. A* **1997**, *101*, 7128–7133.

(63) Huber, H. P.; Herzberg, G. *Constants of diatomic molecules*. Van Nostrand: New York, 1979; p 565.

(64) Ram, R. S.; Bernath, P. F. *J. Chem. Phys.* **1996**, *104*, 6444–6451.

(65) Morgan, J. D., III.; Kutzelnigg, W. *J. Phys. Chem.* **1993**, *97*, 2425–2434.

(66) *NIST Chemistry WebBook, NIST Standard Reference Database Number 69*; Linstrom, P. J., Mallard, W. G., Ed.; National Institute of Standards and Technology: Gaithersburg, MD, 2005.

(67) Adamo, C.; Maldivi, P. *J. Phys. Chem. A* **1998**, *102*, 6812–6820.

(68) Liu, W.; Dolg, M. *Phys. Rev. A: At., Mol., Opt. Phys.* **1998**, *57*, 1721–1728.

(69) Kovács, A.; Konings, R. J. M. *J. Phys. Chem. Ref. Data* **2004**, *33*, 377–404.

(70) Cundari, T. R.; Sommerer, S. O.; Strohecker, L. A.; Tippett, L. *J. Chem. Phys.* **1995**, *103*, 7058–7063.

(71) Adamo, C.; Barone, V. *J. Chem. Phys.* **1999**, *110*, 6158–6170.

(72) Perdew, J. P.; Burke, K.; Ernzerhof, M. *Phys. Rev. Lett.* **1996**, *77*, 3865–3868.

(73) Perdew, J. P.; Burke, K.; Ernzerhof, M. *Phys. Rev. Lett.* **1997**, *78*, 1396–1396.

(74) Perdew, J. P.; Burke, K.; Wang, Y. *Phys. Rev. B* **1996**, *54*, 16533–16539.

(75) Dolg, M.; Liu, W.; Kalvoda, S. *Int. J. Quantum Chem.* **2000**, *76*, 359–370.

(76) Ramakrishnan, R.; Matveev, A. V.; Rösch, N. *Chem. Phys. Lett.* **2009**, *468*, 158–161.

(77) Myers, C. E. *Inorg. Chem.* **1975**, *14*, 199–201.

CT900090F